Prognostic biomarker HIF1α and its correlation with immune infiltration in gliomas

ZIHAN DING[1*], JIAMING ZHANG[2*], LIN LI[1], CHUNLIANG WANG[1] and JINHONG MEI[2,3]

Departments of [1]Neurosurgery and [2]Pathology; [3]Institute of Molecular Pathology, The First Affiliated Hospital, Jiangxi Medical College, Nanchang University, Nanchang, Jiangxi 330006, P.R. China

Received July 27, 2023; Accepted December 6, 2023

DOI: 10.3892/ol.2024.14326

Abstract. Certain glioma subtypes, such as glioblastoma multiforme or low-grade glioma, are common malignant intracranial tumors with high rates of relapse and malignant progression even after standard therapy. The overall survival (OS) is poor in patients with gliomas; hence, effective prognostic prediction is crucial. Herein, the present study aimed to explore the potential role of hypoxia-inducible factor 1 subunit alpha (HIF1α) in gliomas and investigate the association between HIF1α and infiltrating immune cells in gliomas. Data from The Cancer Genome Atlas were evaluated via RNA sequencing, clinicopathological, immunological checkpoint, immune infiltration and functional enrichment analyses. Validation of protein abundance was performed using paraffin-embedded samples from patients with glioma. A nomogram model was created to forecast the OS rates at 1, 3 and 5 years after cancer diagnosis. The association between OS and HIF1α expression was estimated using Kaplan-Meier survival analysis and the log-rank test. Finally, HIF1α expression was validated using western blotting, reverse transcription-quantitative PCR, Cell Counting Kit-8 and Transwell assays. The results demonstrated that HIF1α expression was significantly upregulated in gliomas compared with normal human brain glial cells. Immunohistochemistry staining demonstrated differential expression of the HIF1α protein. Moreover, glioma cell viability and migration were inhibited via HIF1α downregulation. HIF1α impacted DNA replication, cell cycling, DNA repair and the immune microenvironment in glioma. HIF1α expression was also positively associated with several types of immune cells and immunological checkpoints and with neutrophils, plasmacytoid dendritic cells and $CD56^{bright}$ cells. The Kaplan-Meier survival analyses further demonstrated a strong association between high HIF1α expression and poor prognosis in patients with glioma. Analysis of the receiver operating characteristic curves demonstrated that HIF1α expression accurately differentiated paired normal brain cells from tumor tissues. Collectively, these findings suggested the potential for HIF1α to be used as a novel prognostic indicator for patients with glioma and that OS prediction models may help in the future to develop effective follow-up and treatment strategies for these patients.

Correspondence to: Professor Chunliang Wang, Department of Neurosurgery, The First Affiliated Hospital, Jiangxi Medical College, Nanchang University, 17 Yongwaizheng Street, Nanchang, Jiangxi 330006, P.R. China
E-mail: wangchunliang@ncu.edu.cn

Professor Jinhong Mei, Department of Pathology, The First Affiliated Hospital, Jiangxi Medical College, Nanchang University, 17 Yongwaizheng Street, Nanchang, Jiangxi 330006, P.R. China
E-mail: meijinhong@ncu.edu.cn

*Contributed equally

Abbreviations: AUC, area under the curve; BP, biological process; CC, cellular component; CCK-8, cell counting kit-8; DEG, differentially expressed gene; DSS, disease-specific survival; GO, Gene Ontology; GBM, glioblastoma multiforme; GTEx, Genotype-Tissue Expression; HIF1α, hypoxia-inducible factor 1 subunit alpha; HR, hazard ratio; IDH1, isocitrate dehydrogenase 1; IHC, immunohistochemistry; KEGG, Kyoto Encyclopedia of Genes and Genomes; LGG, low-grade glioma; MF, molecular function; NK, natural killer; OS, overall survival; PFI, progression-free interval; RT-qPCR, reverse transcription-quantitative PCR; ROC, receiver operating characteristic; TCGA, The Cancer Genome Atlas; VM, vasculogenic mimicry; WHO, World Health Organization

Key words: hypoxia-inducible factor 1 subunit alpha, glioma, immune infiltration, overall survival prediction model, biomarker

Introduction

In 2016, 227,000 fatalities and 330,000 new cases of central nervous system cancers were reported worldwide (1). Gliomas, which have a high level of heterogeneity and diverse origins, are the most frequently diagnosed primary brain tumors, accounting for 80% of malignant primary tumors in the central nervous system (2). Current standard treatment includes surgical resection, followed by radiotherapy and chemotherapy (3). In the USA, the adjuvant carmustine, a nitrosourea drug, is commonly prescribed (4-6); however, patients with malignant glioma continue to have a poor overall prognosis owing to the high mortality rates (7) and debilitating symptoms. Glioma has been histologically classified from low to high grades by the World Health Organization (WHO) (8-10). Despite substantial research and the use of a combination

of standard therapies, the median survival for patients is still only 14-24 months, with ~10% chance of surviving for 5 years (4,11). Therefore, novel therapeutic strategies are urgently needed. Studies on therapeutic approaches targeting the tumor microenvironment have created new treatment strategies (12). Low-grade gliomas, anaplastic gliomas and glioblastomas have median overall survival (OS) durations of 78.1, 37.6 and 14.4 months, respectively (13). Consequently, prognostic indicators have been investigated to predict patient survival and responsiveness to personalized treatment (14).

Hypoxia-inducible factors (HIFs) belong to a family of DNA-binding transcription factors called basic helix-loop-helix/Per-ARNT-Sim (15). HIF1 is a heterodimeric transcription factor comprising two subunits, HIF1α and HIF1β, each with unique functions (16). HIF1α is an important regulator of gene expression associated with the cellular response to hypoxia (17,18). However, HIF1α promotes carcinogenesis and is a common cancer treatment target (19,20). Notably, HIF1α upregulation enhances the development of certain tumors, including gliomas, breast cancer and prostate cancer, whereas its downregulation inhibits tumor growth (21). The tumor microenvironment, which is crucial for the development, angiogenesis and migration of tumors, has immunosuppressive properties (22). Gliomas actively recruit immune cells by releasing chemokines (23,24) and after entering the tumor environment, immune cells are regulated by immunomodulatory cytokines and molecules, such as TGF-β1 (25). Therefore, tumor-specific immunity is suppressed, while tumor development is promoted by the recruitment of peripheral immune cells into tumors. HIF1α signaling in cancer cells recruits immunosuppressive cells by secreting modulators, thus promoting tumor progression (26). Considering the close association between HIF1α and immune cells, alterations in HIF1α may influence the progression and prognosis of glioma by regulating the level of infiltrating immune cells. However, the relationship between HIF1α and new immune-infiltrating cells needs to be further explored.

Therefore, the present study aimed to investigate the potential role of HIF1α and explore the association between HIF1α and new infiltrating immune cells in gliomas.

Materials and methods

Data extraction and preprocessing. RNA sequencing data were collected from The Cancer Genome Atlas (TCGA)-glioblastoma multiforme (GBM) and TCGA-low-grade glioma (LGG) projects using the Genomic Data Commons Data Portal (https://portal.gdc.cancer.gov) and the Genotype-Tissue Expression (GTEx) databases (http://www.Gtexportal.org/home/) in the transcripts per million format for pan-cancer research. From the TCGA database, data levels 3 HTSeq-FPKM and HTSeq-Count data for GMB/LGG were extracted. The publication requirements of TCGA and GTEx were rigorously adhered to.

Differential expression gene analysis. In the GBM/LGG data, the median HIF1α expression was used as the cutoff value (HTSeq-Count) to distinguish differentially expressed genes (DEGs) between groups with low and high HIF1α expression. An unpaired student's t-test was conducted using the DESeq2 package in R (version 4.3.0) (27).

Pathological specimen selection. A total of 20 paired paraffin-embedded normal tissue samples and glioma specimens were obtained from the Pathology Department of the First Affiliated Hospital of Nanchang University (Nanchang, China). Informed consent was obtained from all patients and ethical approval was obtained from The Medical Ethics Committee of the First Affiliated Hospital of Nanchang University [approval no. (2023)CDYFYYLK(01-018)].

Immunohistochemistry. Immunohistochemical (IHC) staining was used to assess the expression levels of HIF1α in paraffin-embedded tissues obtained from patients with glioma. The tissue samples were subjected to fixation using 4% paraformaldehyde for 24 h at room temperature. Following fixation, the samples were dehydrated through a graded series of alcohol, were subsequently embedded in paraffin, and finally sectioned into 4-μm serial sections. Tissue slides were deparaffinized at 60˚C, and then treated with 100% xylene for 20 min before being rehydrated in a graded series of ethanol at room temperature. Antigen retrieval was conducted in a water bath with 100 ml ethylenediaminetetraacetic acid retrieval buffer (OriGene Technologies, Inc.), at 95˚C, and the sections were then treated with 3% hydrogen peroxide to eliminate endogenous peroxidase for 10 min. Subsequently, the sections were blocked with 5% normal goat serum (cat. no. SL038; Beijing Solarbio Science & Technology Co., Ltd.) at 37˚C for 30 min. The sections were incubated with anti-HIF1α primary antibodies (1:500; cat. no. 20960-1-AP; Proteintech) overnight at 4˚C, followed by incubation with enzyme-labeled Goat Anti-Mouse/Rabbit secondary antibodies (1:100; cat. no. PV-6000D; Beijing Zhongshan Jinqiao Biotechnology Co., Ltd.) at 37˚C for 30 min. Staining was performed using diamino-benzidine (cat. no. PV-6000D; Beijing Zhongshan Jinqiao Biotechnology Co., Ltd.) for 3-5 min at room temperature [both the secondary antibody and DAB were obtained from a kit (cat. no. PV-6000D; Beijing Zhongshan Jinqiao Biotechnology Co., Ltd.)] and a hematoxylin counterstain at room temperature for 20 sec. Brain tissue sections that previously demonstrated positive immunostaining were used as positive controls, whereas samples without the primary antibody staining served as negative controls. A light microscope (ZEISS Axio Lab. A1; CarlZeiss AG) was used to acquire images at x200 and x400 magnifications. Three representative fields of view were examined for each sample. ImageJ Software (version 1.53; National Institutes of Health) was used to determine the average optical density associated with positive expression. The level of expression was evaluated on a scale ranging from 0-7, where 0-2 indicated negative expression and 3-7 indicated positive expression. A score of 3-4 represented weak positive expression and a score of 5-7 denoted strong positive expression. Staining intensity was classified as follows: A score of 0 for no staining, 1 for mild staining, 2 for moderate staining and 3 for intense staining. The scoring for staining area was as follows: A score of 0 for no staining, 1 for staining over 1-25% of the area, 2 for staining over 26-50% of the area, 3 for staining over 51-75% of the area and 4 for staining over 76-100% of the area.

Functional enrichment analysis of HIF1α-related DEGs. The functional enrichment analysis threshold for DEGs was set at |log fold change (FC)|>2 with an adjusted P-value (P adj) <0.05.

The clusterProfiler package in R was used to conduct Gene Ontology (GO) analysis, including molecular functions (MFs), cellular components (CCs) and biological processes (BPs) and Kyoto Encyclopedia of Genes and Genomes (KEGG) pathway enrichment analysis (28,29).

Gene set enrichment analysis. The clusterProfiler R package was used to explore functional and pathway differences between high- and low-HIF1α expression groups (30). Statistical significance for enrichment findings was set at a false discovery rate <0.25 and a P adj <0.05.

Assessment of immune infiltration and immune checkpoints. The single-sample gene set enrichment analysis function in the GSVA R package (31) was used to evaluate HIF1α immunological infiltrates reported in the literature and explore the relationships between HIF1α expression and 24 distinct immune cell subsets (32). The relationships between HIF1α and immunological checkpoints, such as programed cell death protein 1 (PDCD1), CD274, hepatitis A virus cellular receptor 2 (HAVCR2), cytotoxic T-lymphocyte protein 4 (CTLA4), T-cell immunoreceptor with Ig and ITIM domains (TIGIT), lymphocyte activation gene 3 protein (LAG-3) and CD48, were further examined.

Prognostic analysis. Age, sex, WHO grade, isocitrate dehydrogenase 1 (IDH1) mutation status and 1p19q co-deletion status were applied as clinicopathological characteristics in the Cox regression analysis to evaluate the influence of physiological parameters on clinical outcomes. Furthermore, the RMS and survival R packages were used to produce calibration and nomogram plots to estimate the 1-, 3- and 5-year OS rates (33,34). The ability of the nomogram to discriminate between groups was assessed using calibration, receiver operating characteristic (ROC) curves and concordance index methods (35).

Cell culture and cell transfection. The human normal brain glial cell line HEB (cat. no. C449) was acquired from mlbio (Shanghai Enzyme-linked Biotechnology Co., Ltd.), and glioma cell lines U251 (cat. no. AW-CELLS-H0379) and T98G (cat. no. AW-CELLS-H0365) were acquired from AnWei-sci. The U-87 MG cell line is a glioblastoma of unknown origin (cat. no. AW-CELLS-H0381) and was acquired from AnWei-sci. All cells were cultured in high-glucose Dulbecco's modified Eagle's medium (Beijing Solarbio Science & Technology Co., Ltd.) supplemented with 10% fetal bovine serum (FBS; Gibco; Thermo Fisher Scientific, Inc.) and 1% penicillin-streptomycin (Beijing Solarbio Science & Technology Co., Ltd.) at 37˚C and 5% CO_2. All small interfering RNAs (siRNAs), including a negative control (si-NC) and those targeting HIF1α (si-HIF1α), were obtained from HanBio Biotechnology Co., Ltd. The si-HIF1α (5 nM) and si-NC (5 nM) were initially combined with Opti-MEM (Invitrogen; Thermo Fisher Scientific, Inc.), and incubated for 5 min. Subsequently, this mixture was co-incubated with Lipofectamine® 2000 (Invitrogen; Thermo Fisher Scientific, Inc.) for 20 min. The resulting complex was then transfected into the T98G and U87 glioma cell lines and maintained for 6 h at 37˚C and the culture medium was substituted with high-glucose DMEM containing 10% FBS. The following functional experiments were carried out 24 h after transfection. The siRNA sequences were as follows: si-NC sense, 5'-UUCUCCGAACGUGUCACGUTT-3' and antisense, 5'-ACGUGACACGUUCGGAGAATT-3'; and si-HIF1α sense, 5'-GCCGAGGAAGAACUAUGAATT-3' and antisense, 5'-UUCAUAGUUCUUCCUCGGCTT-3'.

Reverse transcription-quantitative PCR (RT-qPCR). The Total RNA Small Amount Extraction kit (Axygen; Corning, Inc.) was used to lyse T98G or U87 cells and extract their total RNA. Prime script RT Master mix (Takara Biotechnology Co., Ltd.) used to reverse transcribe the extracted RNA into cDNA according to the manufacturer's protocol. HIF1α and GAPDH were amplified using primers purchased from Sangon Biotech Co., Ltd. SYBR Green Master Mix (Tiangen Biotech Co., Ltd.) was used for RT-qPCR following the manufacturer's instructions. The thermocycling conditions used for PCR were: Initial denaturation at 95˚C for 10 min, followed by 40 cycles at 95˚C for 15 sec and 60˚C for 60 sec. The $2^{-\Delta\Delta Cq}$ method (36) was used to calculate the relative mRNA expression levels. GAPDH was used as the endogenous control. The primer sequences were as follows: HIF1α forward (F) 5'-GTGGTGGTTACTCAGCACTTT-3' and reverse (R), 5'- ATCTCCGTCCCTCAACCTCT-3'; and GAPDH F, 5'-AGGTCGGTGTGAACGGATTTG-3' and R, 5'-GGGGTCGTTGATGGCAACA-3'.

Protein extraction and western blotting. U87 cells ($2x10^5$ cells/cm^2) and T98G cells ($2x10^5$ cells/cm^2) were lysed using RIPA buffer (cat. no. P0013B; Beyotime Institute of Biotechnology) and PMSF (Beyotime Institute of Biotechnology) with phosphatase inhibitor (Beijing Solarbio Science & Technology Co., Ltd.). The cell lysates were subsequently centrifuged at 15,000 x g for 15 min at 4˚C to isolate the soluble proteins. Proteins were extracted from both cell lysates and supernatants. The BCA Protein Assay Kit (cat. no. P0012; Beyotime Institute of Biotechnology) was used to evaluate the protein concentration of cells. Proteins (20 μg/lane) were separated using 7.5% SDS-PAGE and transferred to polyvinylidene fluoride membranes (Millipore Sigma). The membranes were then blocked using 5% non-fat milk at room temperature for 2 h, and washed with Trisbuffered saline with 0.1% Tween 20 (TBST) and incubated with primary antibodies against HIF1α (1:5,000; cat. no. 20960-1-AP; Wuhan Sanying Biotechnology) and GAPDH (1:20,000; cat. no. 10494-1-AP; Wuhan Sanying Biotechnology) at 4˚C overnight. After the wash with TBST and incubation with goat anti-rabbit IgG (1:10,000; cat. no. BS13278; BioWorld Technology, Inc.) and goat anti-mouse IgG (1:10,000; cat. no. BS12478; BioWorld Technology, Inc.) for 1 h at 25˚C, ECL western blotting substrate (Beijing Solarbio Science & Technology Co., Ltd.) was added to visualize the protein bands using the ChemiDoc XRS molecular imager system (Bio-Rad Laboratories, Inc.). Densitometry was analyzed using ImageJ Software (version 1.53; National Institutes of Health).

Cell Counting Kit-8 (CCK-8) assay. Cell proliferation was investigated using the CCK-8 assay (BIOSS). T98G and U87 cells were transfected with either si-HIF1α or si-NC at 37˚C and 5% CO_2 for 2 days. Subsequently, cells were transferred to 96-well plates (~$2x10^3$ cells/well) and cultured for 1, 2, 3 or 4 days under

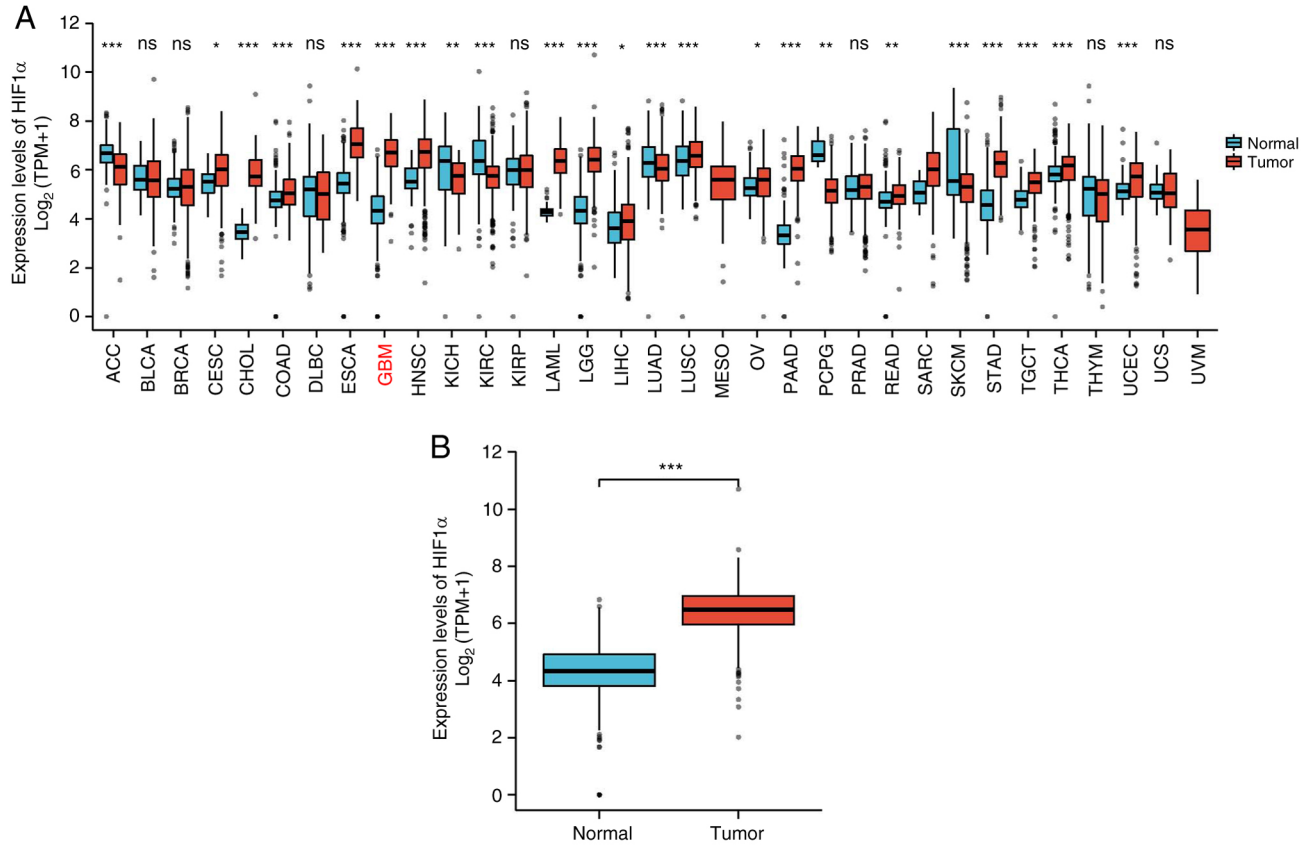

Figure 1. HIF1α expression levels in different tumor samples. HIF1α expression in (A) normal tissues and pan-cancer tissues and (B) glioblastoma multiforme/low-grade glioma samples. *P<0.05, **P<0.01 and ***P<0.001 vs. normal tissue. Ns, not significant; HIF1α, hypoxia-inducible factor 1 subunit alpha.

standard conditions. Cells were incubated with CCK-8 for 2 h and the optical density (450 nm) of each sample was measured using a microplate reader (SpectraMax i3X; Molecular Devices, LLC).

Transwell assay. The upper chamber in the Transwell plate (pore size, 8 μm; Corning Inc.) was filled with 200 μl of serum-free medium and 3x10^4 transfected T98G orU87 cells. Thereafter, 600 μl of complete medium with 5% FBS was added to the lower chamber. After the cells were incubated at 37˚C in 5% CO_2 for 48 h, the Transwell insert was removed and the cells on the upper surface of the membrane were cleared. Cells on the lower surface of the membrane were fixed with 4% paraformaldehyde at room temperature for 30 min, stained with 0.1% crystal violet (Beijing Solarbio Science & Technology Co., Ltd.) at room temperature for 20 min and Images were captured using a light microscope (ZEISS Axio Lab. A1; Carl Zeiss AG) and counted with ImageJ Software (version 1.53; National Institutes of Health).

Statistical analysis. The present study used GraphPad Prism (version 9.3.0; Dotmatics) and R software (version 4.2.1; https://cran.r-project.org/) for conducting all statistical analyses. The Wilcoxon rank-sum test was used for cases where normality tests were not met, while an unpaired Student's t-test was used to assess differences between the two groups when normality tests were satisfied. The Kruskal-Wallis test, a non-parametric test, and one-way ANOVA, a parametric test, were used to compare data across various groups. For ANOVA, a post hoc test (Dunnett's test) was performed if the findings were considered significant, and for the Kruskal-Wallis test, a Dunn's test was utilized. The association between HIF1α expression levels and glioma clinicopathological characteristics was examined using the chi-square test. Kaplan-Meier survival analysis and log-rank tests were used to determine survival distributions. The IHC score was analyzed by a Wilcoxon signed-rank test. The 95% confidence intervals (CIs) and hazard ratios (HRs) for various clinical characteristics were assessed using Cox regression analysis, which identified independent prognostic factors. P<0.05 was considered to indicate a statistically significant difference.

Results

Increased HIF1α expression levels were observed in GBM/LGG. Comparisons of HIF1α expression in tumor samples and healthy tissues from TCGA and GTEx datasets showed that most tumor types exhibited significant upregulation of HIF1α expression (Fig. 1A), including GBM and LGG (P<0.001; Fig. 1B).

To confirm the increased abundance of the HIF1α protein in GBM/LGG tissues compared with that in the corresponding healthy tissues, IHC staining was conducted. Positive staining was primarily observed in the cytoplasm and markedly higher HIF1α expression was observed in glioma tissues compared with matched normal tissues (Fig. 2). Hence, HIF1α was overexpressed in gliomas at the protein level.

HIF1α and functional enrichment analysis for DEG identification. The |logFC|>1.5 and P adj <0.05 criteria were applied

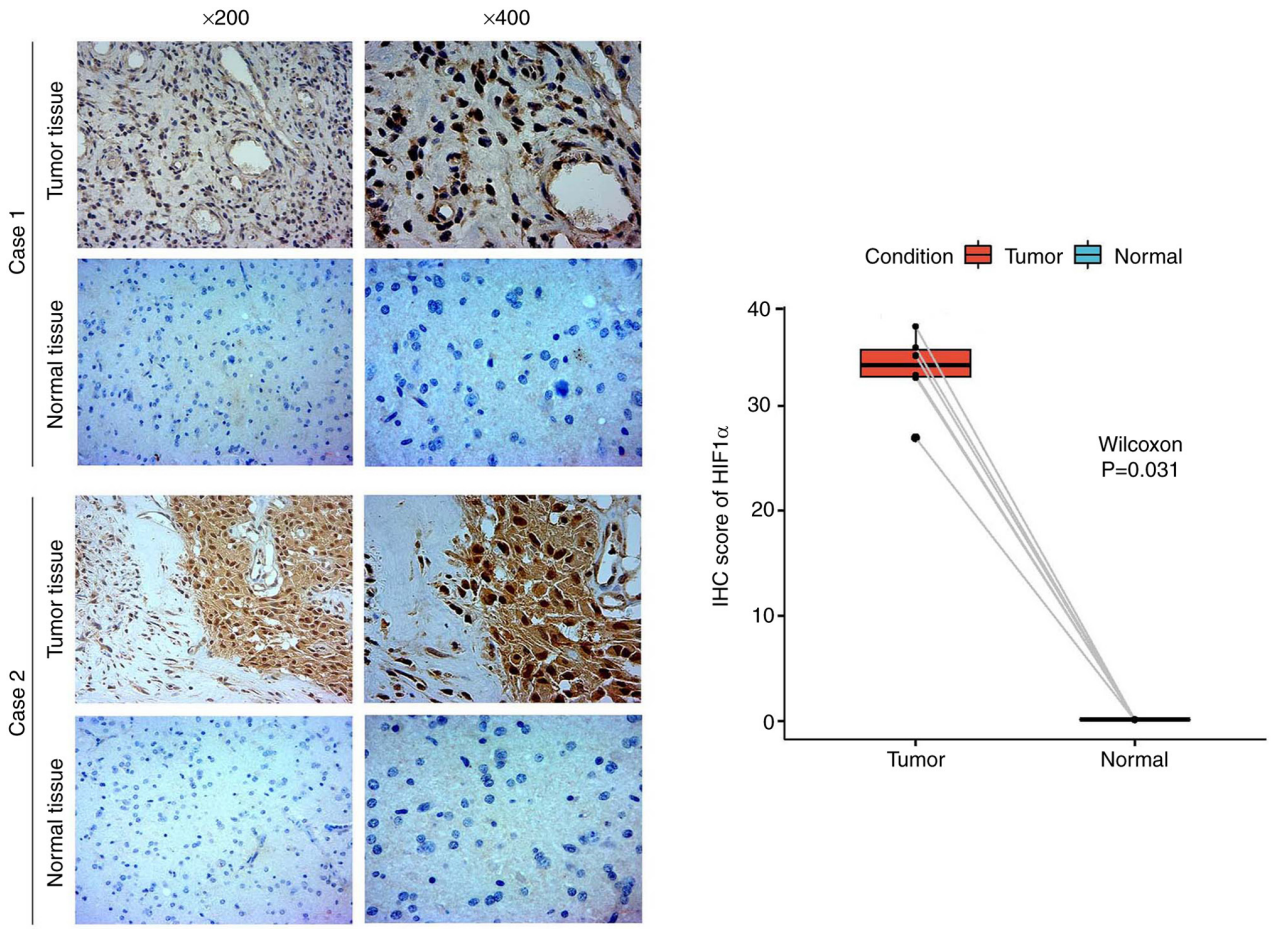

Figure 2. Representative images of HIF1α expression in glioblastoma multiforme/low-grade glioma tissues and their matched normal tissues. Magnification, x200 and x400. HIF1α, hypoxia-inducible factor 1 subunit alpha.

to identify 918 DEGs between two sets of HIF1α samples (low- and high-expression), which comprised 883 upregulated and 35 downregulated genes (Fig. 3A).

GO enrichment analyses demonstrated that the DEGs were enriched in various BPs, including 'nuclear division', 'chromosome segregation', 'mitotic nuclear division' and 'nuclear chromosome segregation'. The enriched CCs included the 'collagen-containing extracellular matrix', 'chromosomal region', 'protein-DNA complex' and 'nucleosome'. The MFs included 'receptor ligand activity', 'DNA-binding transcription activator activity, RNA polymerase', 'cytokine activity' and 'extracellular matrix structural constituents'. KEGG pathway enrichment analysis further demonstrated that the DEGs were associated with 'cytokine-cytokine receptor interaction', 'transcriptional misregulation in cancer', 'systemic lupus erythematosus' and the 'IL-17 signaling pathway' (Fig. 3B).

Gene set enrichment analysis was performed to verify the pathway analyses (Fig. 3C). Clusters associated with cell proliferation exhibited a statistically significant enrichment in HIF1α-related DEGs involving genes related to cell cycle checkpoints, mitotic G1 phase and G1/S transition, DNA replication, cell cycle mitotic and G2/M checkpoints.

Tumor-immune infiltrates and immunological checkpoints in GBM/LGG. Immune cell infiltration is essential for the development of myriad solid tumor types. Analysis of 24 immune cell subtypes in the high- and low-HIF1α expression groups demonstrated that the proportions of T-helper 2 (T_H2), γδT, effector memory T cells (T_{EM}), central memory T cells (T_{CM}), T_H and $CD8^+$ T cells, as well as neutrophils, macrophages, eosinophils and activated dendritic cells (aDCs) were markedly increased in the high-HIF1α group compared with those in the low-HIF1α group (Fig. 4A). By contrast, plasmacytoid dendritic cells (pDCs) and Treg, $CD56^{bright}$ natural killer (NK) and mast cells were significantly downregulated in the high-HIF1α group compared with those in the low-HIF1α group. No significant differences in were observed in B, cytotoxic, $CD56^{dim}$ NK, NK, T, T follicular helper cells (Tfh), THi, T_H17, DCs and interdigitating DCs (iDCs) in the low- and high-expression groups.

Moreover, infiltration of T_H17, T_H2, T_H1, γδT, T_{CM}, T_H, $CD8^+$T cells, neutrophils, macrophages, eosinophils and aDCs was associated with HIF1α expression. By contrast, the infiltration of Treg, $CD56^{bright}$ NK and mast cells and pDCs was inversely associated with HIF1α expression (Figs. 4B and C, S1 and S2). A heat map was used to visualize the association between the ratios of the 24 distinct immune cell subpopulations that permeated the tumors (Fig. 4D).

The relationship between HIF1α expression and immunological checkpoints, including PDCD1, CD274, HAVCR2, CTLA4, TIGIT, LAG-3 and CD48, was also assessed (Fig. 5A).

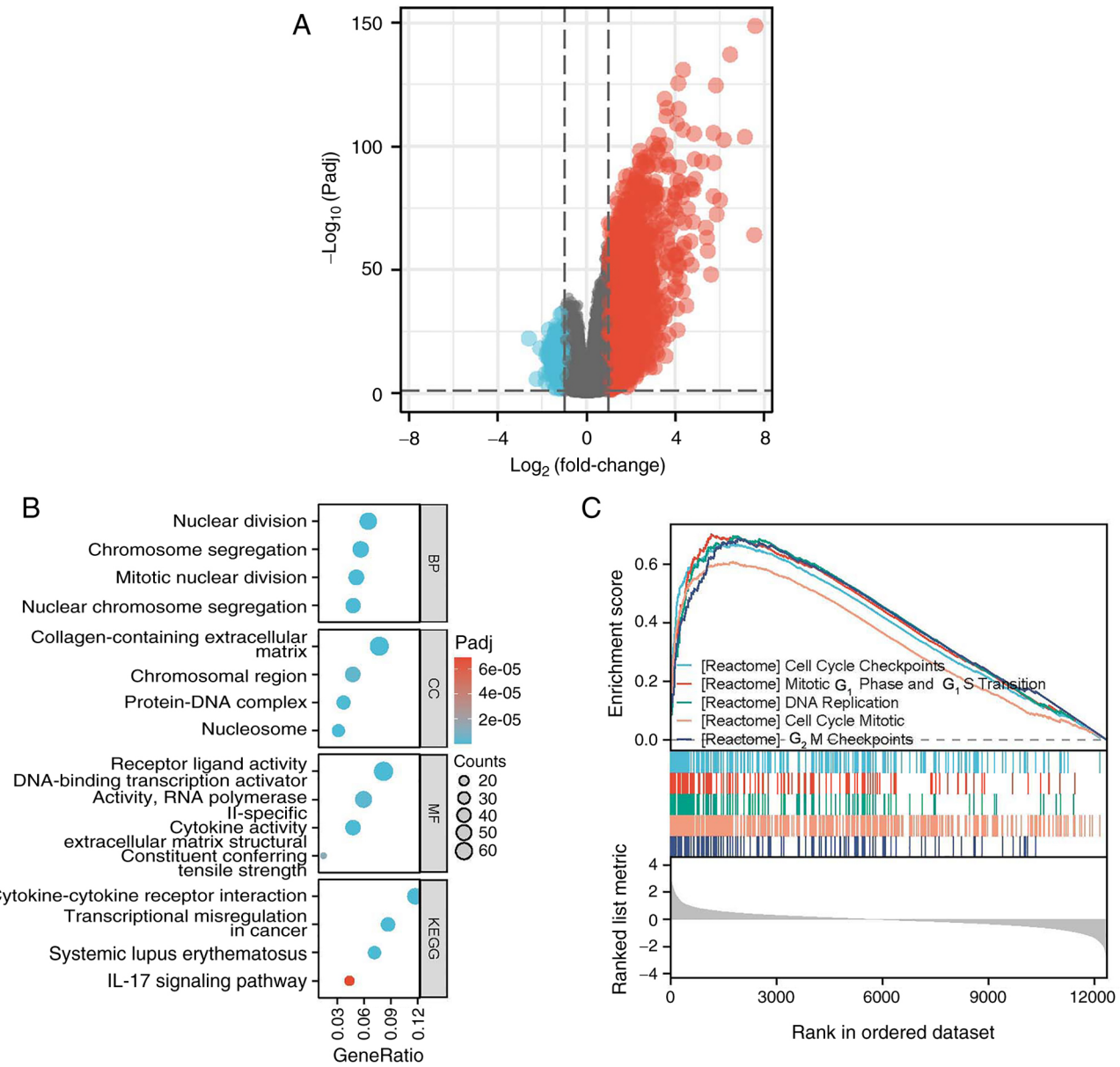

Figure 3. Functional enrichment analyses. (A) Volcano plot of DEGs. (B) Gene Ontology enrichment analysis including biological processes, cellular components and molecular functions and KEGG pathway annotation. (C) Gene set enrichment analysis of DEGs. DEG, differentially expressed genes; P adj, adjusted P-value; BP, biological process; MF, molecular functions; CC, cellular components; KEGG, Kyoto Encyclopedia of Genes and Genomes.

The expression levels of PDCD1, CD274, HAVCR2, LAG-3, TIGIT, CTLA4 and CD48 were positively associated with HIF1α expression levels (P<0.005). The expression levels of these checkpoints were higher in the high-HIF1α group compared with the low-HIF1α group (Fig. 5B). These results suggested that HIF1α serves a crucial role in immune infiltration of gliomas.

Correlation between HIF1α expression and clinical features. The key clinical characteristics between the GBM/LGG low- and high-HIF1α expression groups were compared (Table I). The number of patients with glioblastoma in the IDH1 wild type, 1p/19q non-co-deletion (co-del), WHO G4 and histological type categories were significantly greater in the high-HIF1α expression group compared with the low-HIF1α expression group. Additionally, the expression of HIF1α in relation to other clinical parameters was assessed (Fig. 6). Compared with normal expression levels, HIF1α expression was significantly upregulated in cases of glioblastoma histological type, IDH1 wild type, 1p/19q non-co-deletion and WHO G4.

Relationship between prognostic performance and HIF1α expression levels. The association between HIF1α expression levels and disease-specific survival (DSS), progression-free interval (PFI) and OS in patients with GBM/LGG was evaluated using Kaplan-Meier analysis (Fig. 7). High HIF1α expression levels were associated with a significantly worse prognosis compared with low HIF1α expression (P<0.001). Notably, the PFI (HR=1.30; 95% CI=1.05-1.60; P=0.015; Fig. 7C), DSS (HR=1.45; 95% CI=1.13-1.86; P=0.004; Fig. 7B) and OS (HR=1.34; 95% CI=1.05-1.69; P=0.017; Fig. 7A) were significantly lower in the high-HIF1α expression group compared with the low expression group. The relationships between the risk score, survival time

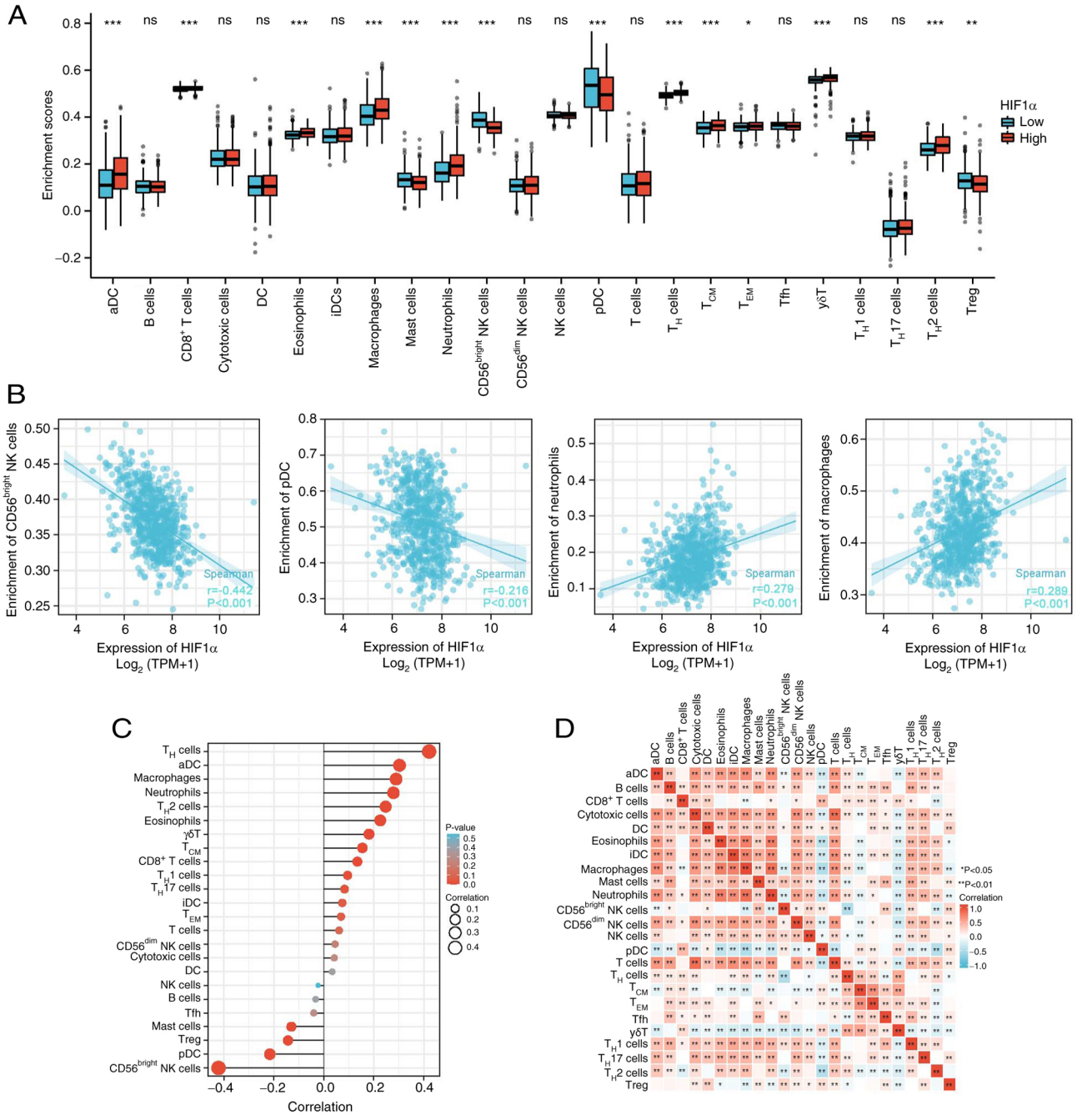

Figure 4. Association between HIF1α expression and immune infiltration in GBM/LGG. (A) The infiltrating levels of 24 immune cell subtypes in high- and low-HIF1α expression groups. Correlation between HIF1α expression and (B) 24 immune cell subtypes or (C) immune infiltration levels. (D) Heatmap of the 24 immune infiltration cells in GBM/LGG. *P<0.05, **P<0.01 and ***P<0.001. GBM/LGG, glioblastoma multiforme/low-grade glioma; HIF1α, hypoxia-inducible factor 1 subunit alpha; ns, not significant.

and HIF1α expression patterns were also examined. Utilizing the risk score, patients with glioma were categorized into two distinct groups. As the risk score increased, there was a concurrent rise in the risk of mortality and a decrease in favorable clinical outcomes for the patients, respectively (Fig. 8).

Age, 1p/19q co-del, WHO grade, IDH1 status, sex and HIF1α expression levels were among the clinical characteristics incorporated in the nomogram model (Fig. 9A). The nomogram demonstrated high therapeutic efficacy for estimating the 1-, 3- and 5-year OS rates of patients with glioma.

The diagnostic utility of HIF1α expression was evaluated using ROC curve analysis. Based on an area under the curve (AUC) of 0.962 (95% CI=0.952-0.972), HIF1α expression demonstrated a statistically significant predictive capacity to differentiate glioma tissues from normal tissues (Fig. 9B). Using calibration plots and time-dependent ROC curves, the likelihood of the 1-, 3- and 5-year OS rates was predicted with AUC values of 0.566, 0.585 and 0.575, respectively. The calibration plots supported the findings of the time-dependent ROC curve analysis. (Fig. 9C and D).

Prognostic value of HIF1α within the specific clinical parameters of gliomas. The predictive value of HIF1α was determined by analyzing specific clinical parameters,

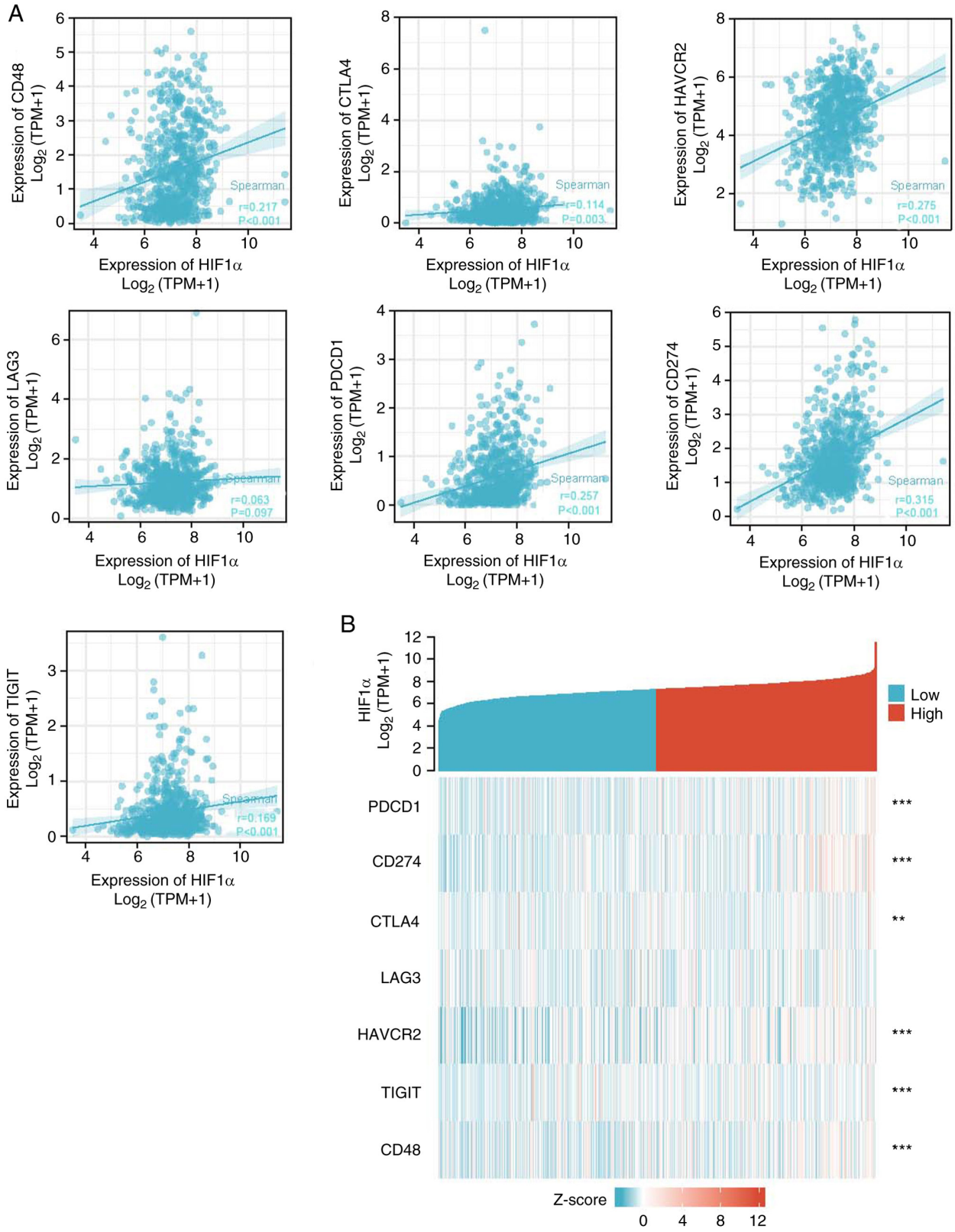

Figure 5. Association between HIF1α expression and immune checkpoints. (A) Correlation between HIF1α expression and immune checkpoints. (B) Heat map of the expression levels of immune checkpoints. **P<0.01 and ***P<0.001. HIF1α, hypoxia-inducible factor 1 subunit alpha; CTLA4, cytotoxic T-lymphocyte protein 4; HAVCR2, hepatitis A virus cellular receptor 2; LAG3, lymphocyte activation gene 3 protein; PDCD1, programed cell death protein 1; TIGIT, T-cell immunoreceptor with Ig and ITIM domains.

including WHO grade, IDH1 status, 1p/19q, sex, ethnicity and histological type (Fig. 10). Elevated HIF1α expression levels correlated with adverse OS in patients with glioma for four clinical parameters: Ethnicity, white and African-American (hazard ratio [HR]=1.29; P=0.041); sex, female (HR=1.51; P<0.05); age, ≤60 years (HR=1.49; P<0.005); and clinical

Table I. Association between HIF1α expression levels and clinicopathologic features in glioblastoma multiforme/low-grade glioma.

Characteristic	Low expression level of HIF1α	High expression level of HIF1α	P-value
Total number of patients, n	348	348	
Sex, n (%)			0.193
Female	158 (22.7%)	140 (20.1%)	
Male	190 (27.3%)	208 (29.9%)	
Histological type, n (%)			<0.001
Astrocytoma	101 (14.5%)	94 (13.5%)	
Glioblastoma	61 (8.8%)	107 (15.4%)	
Oligoastrocytoma	77 (11.1%)	57 (8.2%)	
Oligodendroglioma	109 (15.7%)	90 (12.9%)	
World Health Organization grade, n (%)			<0.001
G2	131 (20.6%)	93 (14.6%)	
G3	123 (19.4%)	120 (18.9%)	
G4	61 (9.6%)	107 (16.9%)	
Isocitrate dehydrogenase status, n (%)			0.010
Wild type	106 (15.5%)	140 (20.4%)	
Mutated	236 (34.4%)	204 (29.7%)	
1p/19q co-deletion, n (%)			0.007
Co-deletion	102 (14.8%)	69 (10%)	
Non-co-deletion	245 (35.6%)	273 (39.6%)	
Age, median (interquartile range)	44.5 (35, 58)	46.5 (34, 59)	0.809[a]

Data were analyzed using the χ^2 test or [a]Wilcoxon rank-sum test. HIF1α, hypoxia-inducible factor 1 subunit alpha.

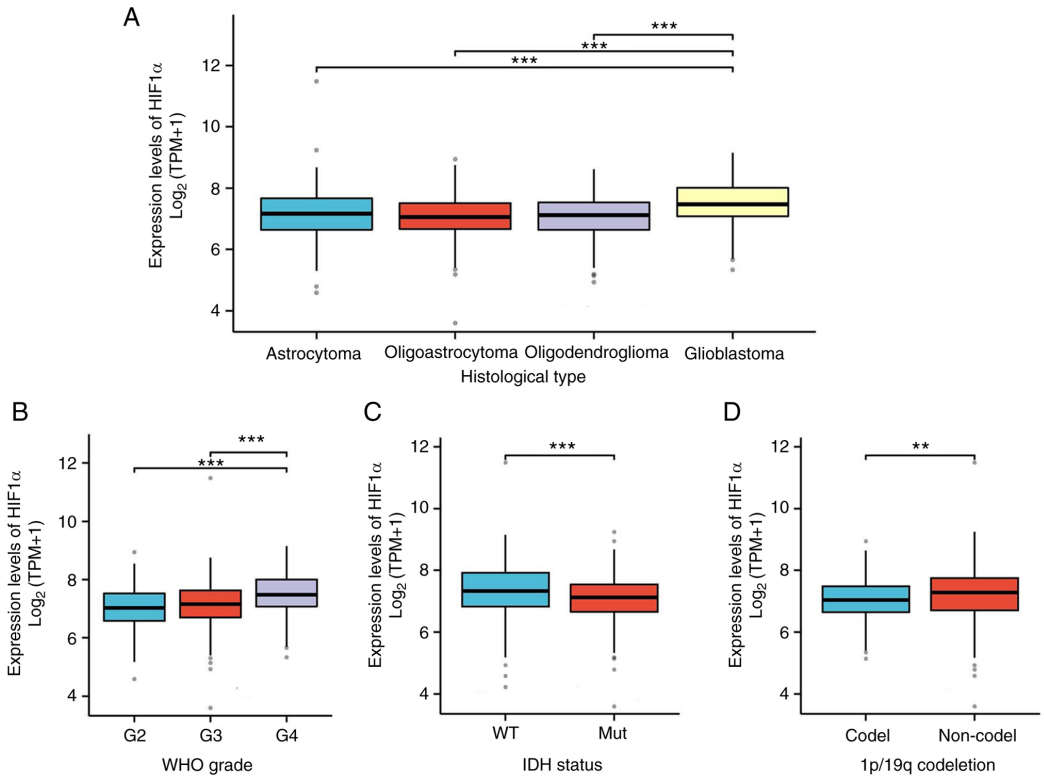

Figure 6. Association between HIF1α expression and clinical features. (A) Expression level of HIF1α in different histology types. (B) Expression level of HIF1α in different WHO grades. (C) Expression level of HIF1α in different IDH mutation statuses. (D) Expression level of HIF1α in different 1p19q codeletion statuses. The statistical methods used were the Kruskal-Wallis test and Dunn' test (A and B) and the Wilcoxon rank-sum test (C and D). **P<0.01 and ***P<0.001. HIF1α, hypoxia-inducible factor 1 subunit alpha; WHO, World Health Organization; IDH, isocitrate dehydrogenase. Co-del, co-deletion.

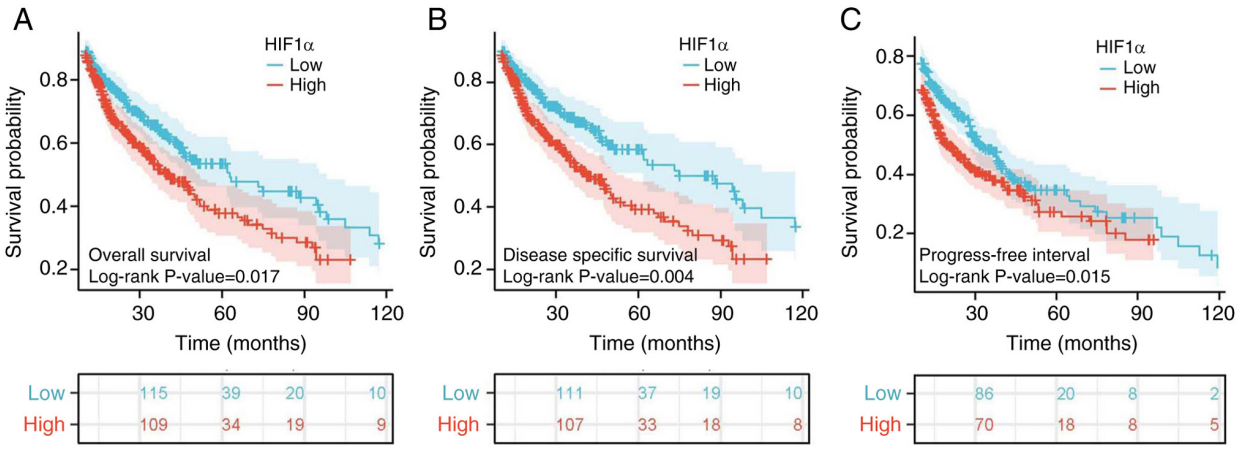

Figure 7. HIF1α prognostic predictive value in patients with glioma. Kaplan-Meier survival analysis showing differences in (A) overall survival, (B) disease-specific survival and (C) progression-free interval of patients with GBM/LGG with high and low HIF1α expression. Survival curves represent patients with GBM/LGG with high (red) and low (blue) HIF1α expression. P<0.05 indicated a statistically significant difference. GBM/LGG, glioblastoma multiforme/low-grade glioma; HIF1α, hypoxia-inducible factor 1 subunit alpha.

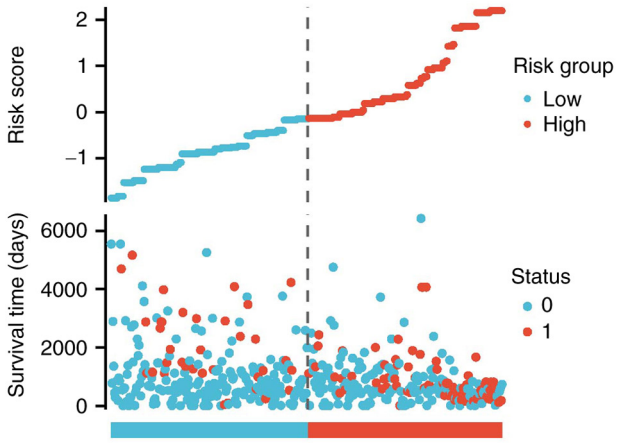

Figure 8. Risk score distribution and survival status of patients. High and low risk scores were determined based on the median risk score. 0, deceased; 1, alive.

histologic types, oligoastrocytoma, oligodendroglioma and glioblastoma (HR=1.44; P=0.008; Fig. 10A). Unfavorable DSS correlated with high HIF1α expression levels for five clinical parameters: 1p/19q, no-co-del (HR=1.32; P=0.043); ethnicity, white and African-American (HR=1.39; P=0.011); sex, female (HR=1.72; P<0.005); age, ≤60 years (HR=1.53; P<0.005); and clinical histologic types, oligoastrocytoma, oligodendroglioma and glioblastoma (HR=1.58; P=0.002; Fig. 10B). In addition, high HIF1α expression was associated with poor PFI for four clinical parameters: 1p/19q, no-co-del (HR=1.31; P=0.022); sex, female (HR=1.46; P=0.025); ethnicity, white and African-American (HR=1.28; P=0.023); and clinical histologic types, oligoastrocytoma, oligodendroglioma and glioblastoma (HR=1.43; P=0.004; Fig. 10C). Therefore, patients with gliomas expressing high HIF1α levels demonstrated a significantly lower survival rate compared with patients with low HIF1α expression levels.

Knockdown of HIF1α expression by siRNA transfection inhibits glioma cell growth and migration. To investigate the functional role of HIF1α in glioma cells, the expression levels of HIF1α were detected in both glioma cell lines (T98G, U87 and U251) and normal brain tissue cells (HEB). HIF1α mRNA (Fig. 11A) and protein (Fig. 11B) expression levels were significantly higher in GBM cells compared with normal brain tissue cells. si-HIF1α significantly suppressed endogenous HIF1α expression in two glioma cell lines (T98G and U87), whereas HIF1α expression remained unaffected in si-NC-transfected cells (Fig. 11C and D). The CCK-8 assay was used to assess cell proliferation (Fig. 11E). The proliferative capacities of HIF1α-knockdown T98G and U87 cells were significantly inhibited compared with those of si-NC-transfected cells on days 3 and 4 following transfection. Additionally, HIF1α knockdown significantly decreased the migration of T98G and U87 GBM cells (Fig. 11F).

These results indicated that siHIF1α effectively reduced HIF1α expression and inhibited glioma cell growth and migration. Mechanistically, this may potentially be caused by the reduction of microvascular mimicry by silencing HIF1α expression, thus inhibiting glioma growth.

Discussion

HIF1α is abundantly expressed in several types of malignancies and has been linked to various cancer features, including metastasis, stimulation of tumor formation, invasion via angiogenesis and modulation of cellular metabolism in hypoxic tumor microenvironments (26,37). PRMT3 has previously been reported to accelerate the development of gliomas by promoting HIF1α-mediated glycolysis and metabolic rewiring (38). Moreover, HIF1α and programmed death-ligand 1 (PD-L1) are positively associated with gliomas. Therefore, targeting HIF1α can improve the effectiveness of anti-PD-1/PD-L1 therapies for gliomas (39). Mechanistically, HIF1α promotes chemoresistance by enabling the dedifferentiation of normal glioma cells and preserving glioma stem cell stemness (40). Additionally, HIF1α is expressed by various immune cells, including macrophages, neutrophils, dendritic cells, and lymphocytes, and modulates innate and adaptive immunity within the tumor microenvironment (26,41,42). To assess the predictive

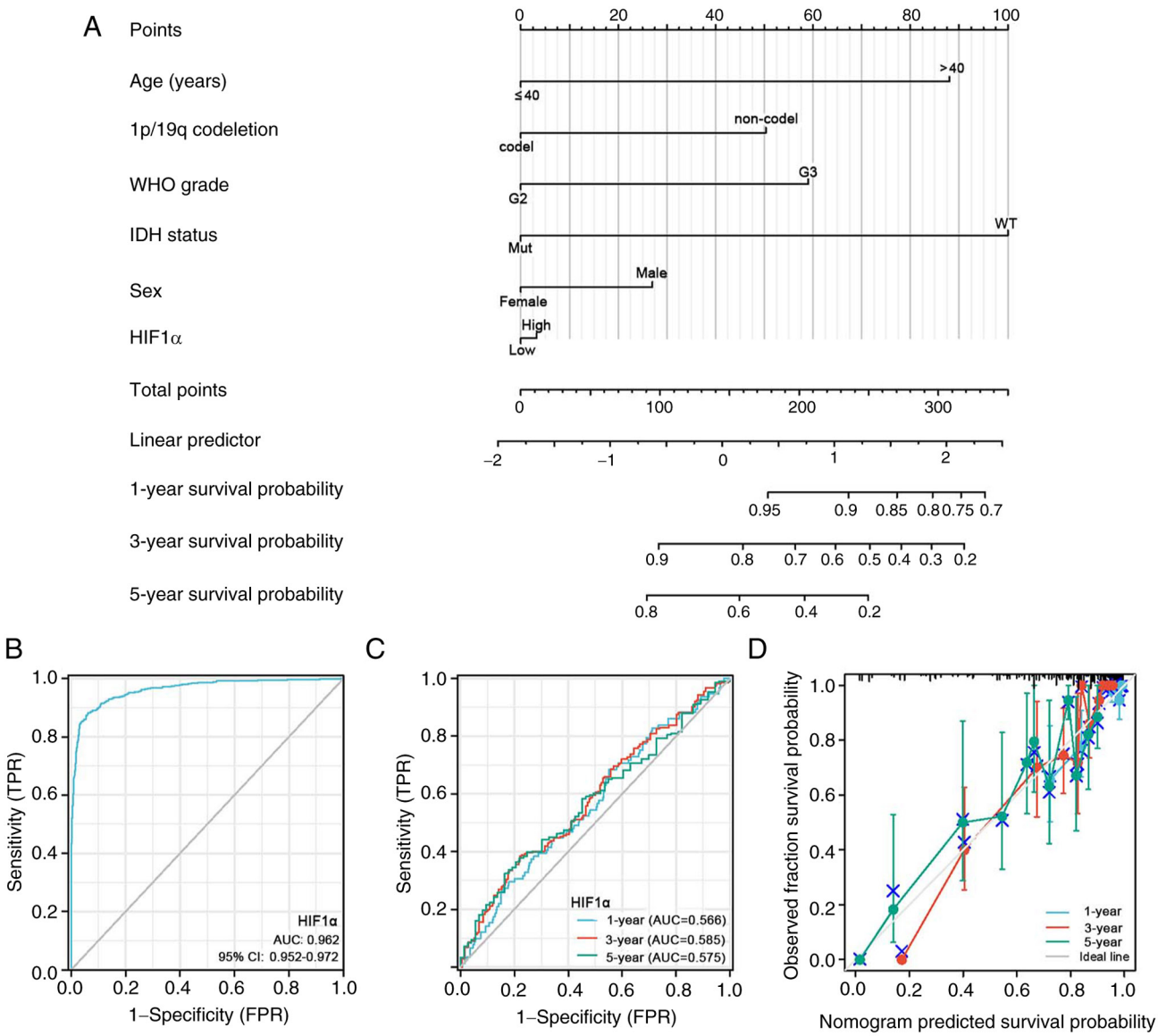

Figure 9. Prognostic prediction model of HIF1α expression in patients with glioblastoma multiforme/low-grade glioma. (A) Nomogram of the 1-, 3- and 5-year overall survival rates. (B) Diagnostic ROC curve of HIF1α. (C) Time-dependent ROC curves and AUC values and (D) calibration plots for 1-, 3- and 5-year OS prediction. ROC, receiver operating characteristic; WHO, World Health Organization; IDH, isocitrate dehydrogenase; HIF1α, hypoxia-inducible factor 1 subunit alpha; AUC, area under the curve; mut, mutated; WT, wild type; FPR, false positive rate; TPR, true positive rate.

significance of HIF1α, data were collected from the TCGA database and the expression patterns of HIF1α in gliomas were evaluated. The results of the present study provided a potential theoretical basis for the development of personalized treatment strategies for patients with glioma. Therefore, characterizing the clinical and molecular relationships between HIF1α expression and glioma malignancy may potentially identify viable therapeutic targets and provide insights into glioblastoma treatment. According to the findings of the present study, immune infiltration and OS were significantly associated with HIF1α expression in patients with GBM/LGG.

In the present study, HIF1α expression levels were compared across several types of cancers. In most cancer types analyzed, including GBM/LGG, HIF1α expression was significantly upregulated compared with that in normal tissues. Moreover, glioma tissues exhibited upregulation of HIF1α-associated DEGs involved in DNA replication, DNA damage repair and the cell cycle. DNA is a fundamental feature of tumor cell proliferation and is closely related to the cell cycle process (43). The proliferation of cells in gliomas may thus be influenced by upregulated HIF1α expression. Additionally, DNA repair promotes chemotherapeutic resistance in tumor cells while ensuring cell survival (44). Therefore, downregulating HIF1α expression may cause cells to enter a state of defective DNA repair, which may prove advantageous for patients with chemotherapy-resistant gliomas. Tumor-specific immunotherapy modifies the immune system to treat a range of cancers (45-47). The gene function enrichment findings in the present study suggested that HIF1α alterations may impact the glioma immune microenvironment.

Furthermore, the expression of HIF1α mRNA was positively associated with the proportion of certain immune cells, such as T_H17, T_H2, T_H1 and $CD8^+$ T cells. Tumors with high HIF1α expression were heavily infiltrated by immune

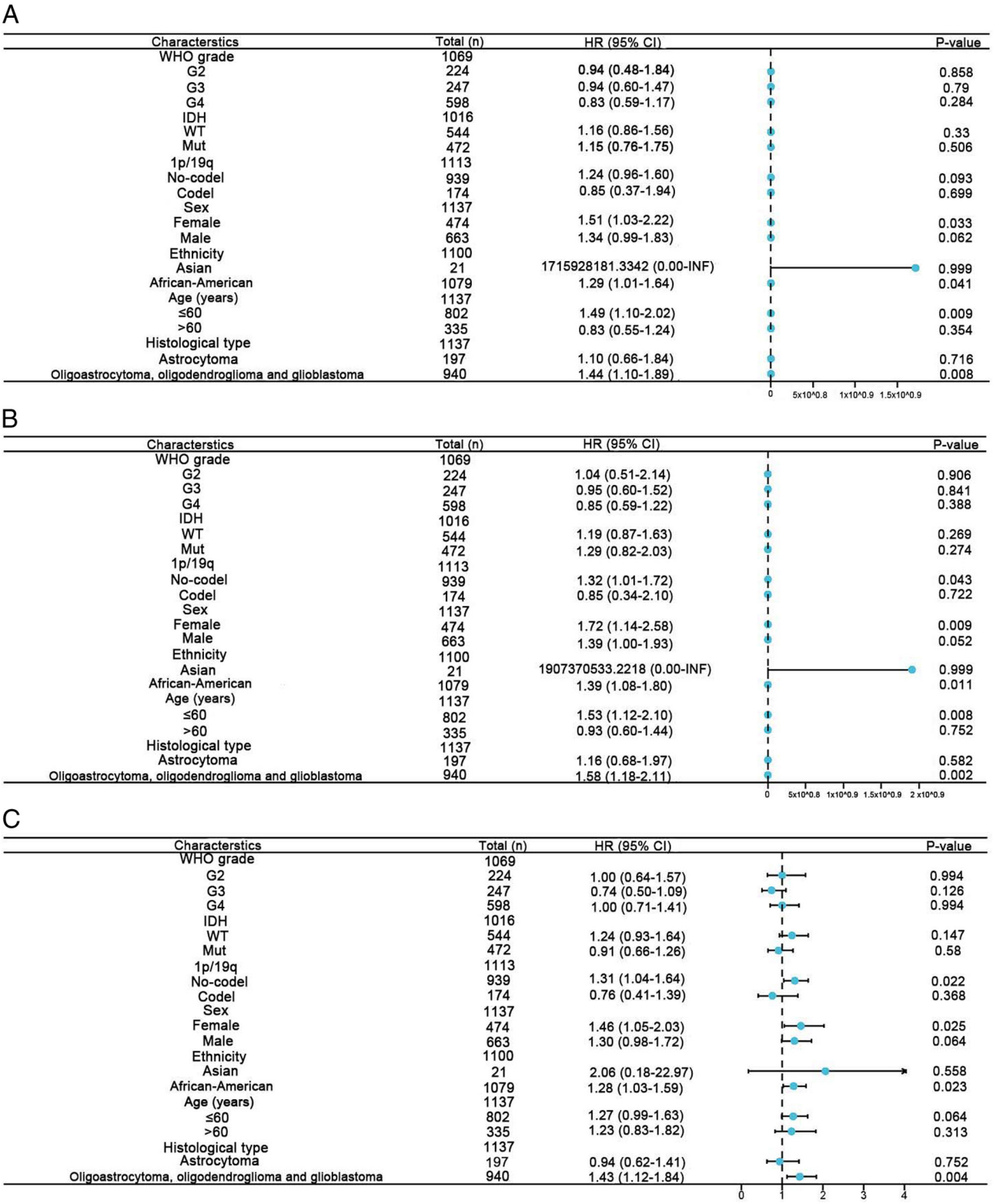

Figure 10. Association between HIF1α expression and (A) overall survival, (B) disease-specific survival and (C) progression-free interval in patients with glioma with specific clinical features. HIF1α, hypoxia-inducible factor 1 subunit alpha; WHO, World Health Organization; IDH, isocitrate dehydrogenase; WT, wild type; mut, mutated; HR, hazard ratio.

cells. Previous studies have reported that the stabilization of expression of HIF1α in macrophages (48), T_H17 cells (49), $CD8^+$ T cells (50) and T_H1 cells (51) influences glioma progression, which was corroborated by the results of the present study. The present study also demonstrated that HIF1α expression was positively associated with the presence of neutrophils. Tumor-associated neutrophils may facilitate invasion and migration of tumor cells (52-54), while increased neutrophil recruitment during antiangiogenic therapy accelerates the development of gliomas and may contribute to

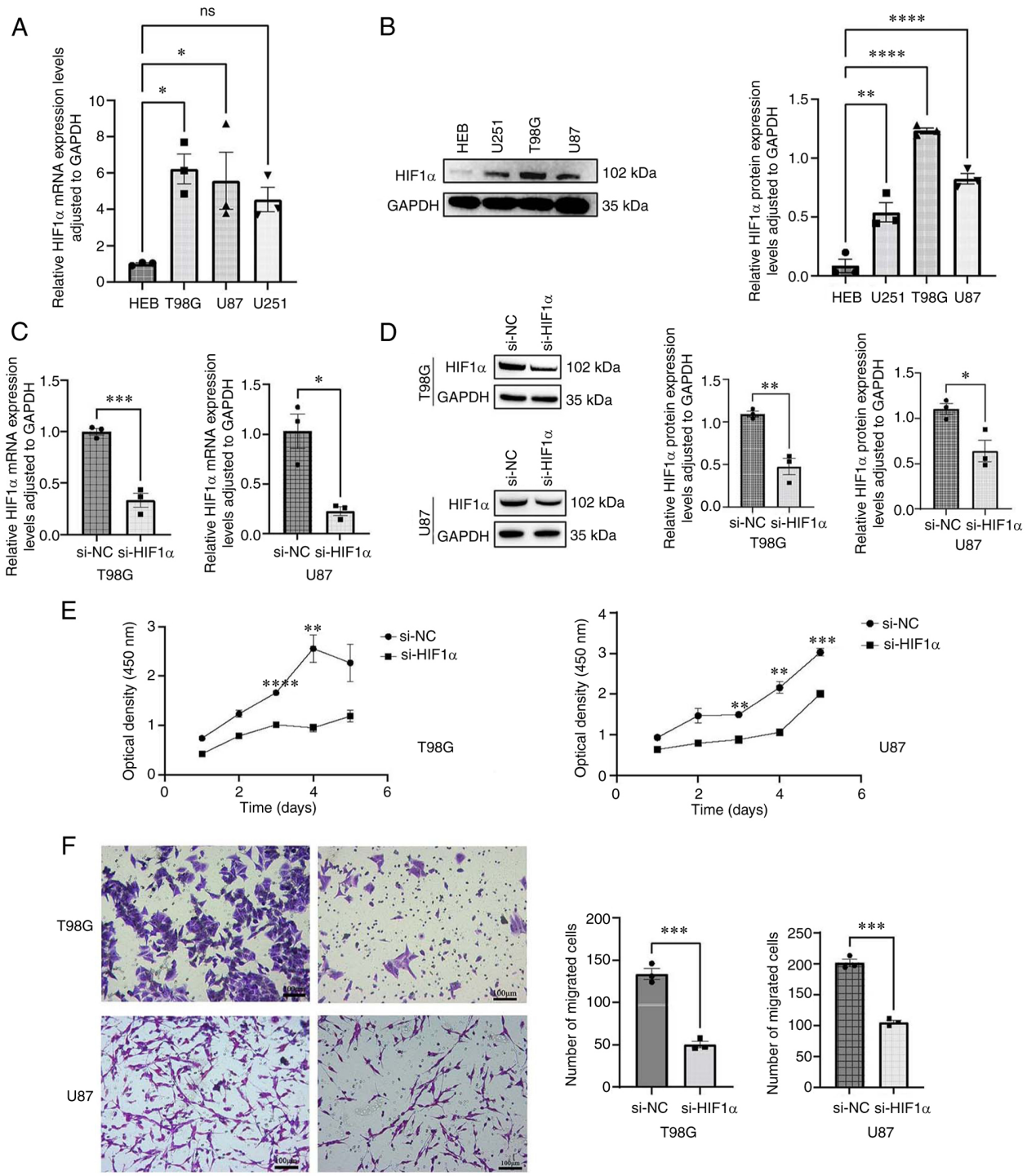

Figure 11. Upregulation of HIF1α in GBM cells and the migratory capacity of cells *in vitro*. (A) RT-qPCR analysis of HIF1α expression in GBM cells. (B) Western blotting analysis of HIF1α abundance in GBM cells. (C) RT-qPCR verification of siRNA efficiency. (D) Western blotting verification of siRNA efficiency. (E) Cell Counting Kit-8 assay of GBM proliferation following HIF1α knockdown. (F) Transwell assay of GBM migration following HIF1α knockdown. Scale bar, 100 μm. Data are presented as mean ± standard error of the mean (n=3). *P<0.05, **P<0.01, ***P<0.001, ****P<0.0001. Data were analyzed using one-way ANOVA followed by a post hoc test (Dunnett's test) for (A and B) or a two-tailed unpaired Student's t-test for (C-F). GBM, glioblastoma multiforme; HIF1α, hypoxia-inducible factor 1 subunit alpha; RT-qPCR, reverse transcription-quantitative PCR; si, small interfering RNA; ns, no significance; NC, negative control.

treatment resistance (55). In glioblastoma, the present study demonstrated an association between HIF1α expression and CD56^{bright} NK cells and pDCs. Innate immunological defense against cancer relies on NK cells (56). Meanwhile, IFN-I generated by pDCs exhibits anticancer properties (57). Owing to the inverse relationship between CD56^{bright} NK cells and HIF1α expression observed in the present study, the infiltration of CD56^{bright} NK cells into solid tumors was relatively minimal compared with other types of immune cells. The primary function of CD56^{bright} NK cells is immunomodulation via the generation of a myriad of cytokines (58,59). This may result in an antitumor effect and deregulation of tumor

immunosurveillance. HIF1α expression may be modified in these cells and thus influence glioma progression. Additionally, the present study demonstrated a positive relationship between HIF1α expression and immunological checkpoints, namely PDCD1, CTLA4, CD274, HAVCR2, TIGIT, LAG-3 and CD48. CTLA-4 and PDCD-1 are critical proteins associated with tumor immune escape (60,61). Ipilimumab, a CTLA-4 inhibitor, and nivolumab, a PDCD-1 inhibitor, are immune checkpoint inhibitors (ICIs) that increase the OS rates of patients with melanoma (62,63). Hence, HIF1α may impact tumor immunology, making it an immunological target rather than merely a prognostic indicator.

In the future, a treatment combination of HIF1α inhibitors with ICIs utilizing the features of HIF1α that enhance the proportions of macrophages and neutrophils while decreasing the proportions of $CD56^{bright}$ NK cells and pDCs could be leveraged, thus improving the therapeutic effects of immunotherapy in patients with gliomas. The results of the present study indicated that HIF1α alteration may affect the progression and prognosis of glioma by regulating the levels of infiltrating immune cells. Wild type IDH1, 1p/19q non-deletion and WHO G4 ratios were significantly increased in patients with elevated HIF1α expression, which suggested a potential role for HIF1α as a positive prognostic predictor. Hence, the predictive potential of HIF1α in patients with GBM/LGG was further investigated.

Using Kaplan-Meier survival analysis, it was demonstrated that HIF1α expression was related to PFI, DSS and OS, which suggested that high HIF1α expression may be associated with adverse results in patients with GBM/LGGs, with specific associations detected with clinical features including IDH1 status, 1p/19q, sex, ethnicity and histological type. These results demonstrated the possible potential of HIF1α as a diagnostic and predictive indicator of gliomas. To further evaluate the 1-, 3- and 5-year OS rates of GBM/LGG, a nomogram prognostic model based on HIF1α expression levels was developed. HIF1α expression greatly enhanced the prognostic evaluation of patients with gliomas. Calibration plots, ROC curves and time-dependent ROC curves confirmed the accurate predictive ability of the nomogram. The methodology presented in the present study offers a novel perspective on the evaluation and prediction of outcomes in patients with GBM/LGG, while providing insights into the progression of gliomas, new therapeutic targets and prognostic indicators.

Furthermore, the present study confirmed that HIF1α was highly expressed in GBM cells and contributed to their migratory abilities. El-Naggar *et al* (64) reported that the ability of sarcoma cells to metastasize may be increased by overexpressing HIF1α. Similarly, HIF1α can regulate breast cancer metastasis, promoting its development (65). The present study demonstrated that HIF1α promoted the migration and, thus, the malignancy of GBM cells. Vasculogenic mimicry (VM) reportedly contributes to the growth of many tumor types, including breast cancer (66), liver cancer (67) and glioma (68). Under hypoxic conditions, the mammalian target of rapamycin participates in VM development in gliomas via HIF1α (69). By contrast, B cell lymphoma 2 inhibits the formation of VM in gliomas by suppressing HIF1α-matrix metalloprotease (MMP)-2-MMP-14 signaling pathway activation (70). Therefore, mechanistically, HIF1α silencing may reduce cell proliferation and migration by inhibiting microvascular mimicry, thereby inhibiting glioma progression. This further demonstrates the potential of HIF1α as a target for the future diagnosis and treatment of malignancies.

The present study has several limitations. The molecular mechanisms underlying the effects of HIF1α silencing on cell migration and proliferation in glioma cells were not experimentally validated. *In vivo* experiments are warranted to verify the correlation between HIF1α expression and glioma development and elucidate the underlying molecular mechanisms. In addition, temporary transfection was performed. Hence, future studies should use stable transfection trials to evaluate the associated impact of HIF1α knockdown. Moreover, clinical studies are required to evaluate the relationship between HIF1α expression, clinical characteristics and patient prognosis, which may aid in the potential identification of novel markers for monitoring tumor growth, accelerate the development of new drugs and enhance future treatment approaches.

The findings of the present study suggested that poor prognosis in GBM/LGGs was associated with HIF1α overexpression. HIF1α may affect the proliferation and metastasis of gliomas by regulating infiltrating immune cells, including neutrophils, pDCs and $CD56^{bright}$ cells. Hence, HIF1α may be a potentially promising independent predictive factor and potential candidate for the treatment of GBM/LGGs.

Acknowledgements

Not applicable.

Funding

This work was funded by The National Natural Science Foundation of China (grant no. 82260525), The Key Program of the National Natural Science Foundation of Jiangxi Province (grant no. 20212ACB206015) and The Science and Technology Project of the Jiangxi Provincial Health Commission (grant no. 202130174).

Availability of data and materials

The datasets used and/or analyzed during the current study are available from the corresponding author on reasonable request.

Authors' contributions

JM and CW designed the study and confirm the authenticity of all the raw data. ZD, JZ and LL gathered and evaluated the data and prepared the manuscript. ZD and JZ edited the manuscript. ZD performed the experiments. All authors read and approved the final version of the manuscript.

Ethics approval and consent to participate

This study was approved by the medical ethics committees of the First Affiliated Hospital of Nanchang University [approval no. (2023)CDYFYYLK(01-018)].

Patient consent for publication

Not applicable.

Competing interests

The authors declare that they have no competing interests.

References

1. GBD 2016 Brain and Other CNS Cancer Collaborators: Global, regional, and national burden of brain and other CNS cancer, 1990-2016: A systematic analysis for the global burden of disease study 2016. Lancet Neurol 18: 376-393, 2019.
2. Weller M, Wick W, Aldape K, Brada M, Berger M, Pfister SM, Nishikawa R, Rosenthal M, Wen PY, Stupp R and Reifenberger G: Glioma. Nat Rev Dis Primers 1: 15017, 2015.
3. Ma R, Taphoorn MJB and Plaha P: Advances in the management of glioblastoma. J Neurol Neurosurg Psychiatry 92: 1103-1111, 2021.
4. Stupp R, Mason WP, van den Bent MJ, Weller M, Fisher B, Taphoorn MJ, Belanger K, Brandes AA, Marosi C, Bogdahn U, *et al*: Radiotherapy plus concomitant and adjuvant temozolomide for glioblastoma. N Engl J Med 352: 987-996, 2005.
5. Jiang T, Nam DH, Ram Z, Poon WS, Wang J, Boldbaatar D, Mao Y, Ma W, Mao Q, You Y, *et al*: Clinical practice guidelines for the management of adult diffuse gliomas. Cancer Lett 499: 60-72, 2021.
6. Stupp R, Brada M, van den Bent MJ, Tonn JC and Pentheroudakis G; ESMO Guidelines Working Group. High-grade glioma: ESMO clinical practice guidelines for diagnosis, treatment and follow-up. Ann Oncol 25 (Suppl 3): iii93-iii101, 2014.
7. Ferlay J, Colombet M, Soerjomataram I, Mathers C, Parkin DM, Pineros M, Znaor A and Bray F: Estimating the global cancer incidence and mortality in 2018: GLOBOCAN sources and methods. Int J Cancer 144: 1941-1953, 2019.
8. Daumas-Duport C, Scheithauer B, O'Fallon J and Kelly P: Grading of astrocytomas. A simple and reproducible method. Cancer 62: 2152-2165, 1988.
9. Louis DN, Perry A, Reifenberger G, von Deimling A, Figarella-Branger D, Cavenee WK, Ohgaki H, Wiestler OD, Kleihues P and Ellison DW: The 2016 world health organization classification of tumors of the central nervous system: A summary. Acta Neuropathol 131: 803-820, 2016.
10. Cancer Genome Atlas Research Network, Brat DJ, Verhaak RG, Aldape KD, Yung WK, Salama SR, Cooper LAD, Rheinbay E, Miller CR, Vitucci M, *et al*: Comprehensive, integrative genomic analysis of diffuse lower-grade gliomas. N Engl J Med 372: 2481-2498, 2015.
11. Stummer W, Meinel T, Ewelt C, Martus P, Jakobs O, Felsberg J and Reifenberger G: Prospective cohort study of radiotherapy with concomitant and adjuvant temozolomide chemotherapy for glioblastoma patients with no or minimal residual enhancing tumor load after surgery. J Neurooncol 108: 89-97, 2012.
12. Jain RK, Martin JD and Stylianopoulos T: The role of mechanical forces in tumor growth and therapy. Annu Rev Biomed Eng 16: 321-346, 2014.
13. Yang P, Wang Y, Peng X, You G, Zhang W, Yan W, Bao Z, Wang Y, Qiu X and Jiang T: Management and survival rates in patients with glioma in China (2004-2010): A retrospective study from a single-institution. J Neurooncol 113: 259-266, 2013.
14. Wang S, Wu W, Lin X, Zhang KM, Wu Q, Luo M and Zhou J: Predictive and prognostic biomarkers of bone metastasis in breast cancer: Current status and future directions. Cell Biosci 13: 224, 2023.
15. Greer SN, Metcalf JL, Wang Y and Ohh M: The updated biology of hypoxia-inducible factor. EMBO J 31: 2448-2460, 2012.
16. Kenneth NS and Rocha S: Regulation of gene expression by hypoxia. Biochem J 414: 19-29, 2008.
17. Wang GL, Jiang BH, Rue EA and Semenza GL: Hypoxia-inducible factor 1 is a basic-helix-loop-helix-PAS heterodimer regulated by cellular O2 tension. Proc Natl Acad Sci USA 92: 5510-5514, 1995.
18. Iyer NV, Kotch LE, Agani F, Leung SW, Laughner E, Wenger RH, Gassmann M, Gearhart JD, Lawler AM, Yu AY and Semenza GL: Cellular and developmental control of O2 homeostasis by hypoxia-inducible factor 1 alpha. Genes Dev 12: 149-162, 1998.
19. Keith B, Johnson RS and Simon MC: HIF1α and HIF2α: Sibling rivalry in hypoxic tumour growth and progression. Nat Rev Cancer 12: 9-22, 2011.
20. Semenza GL: Hypoxia-inducible factors in physiology and medicine. Cell 148: 399-408, 2012.
21. Semenza GL: Defining the role of hypoxia-inducible factor 1 in cancer biology and therapeutics. Oncogene 29: 625-634, 2010.
22. Polyak K, Haviv I and Campbell IG: Co-evolution of tumor cells and their microenvironment. Trends Genet 25: 30-38, 2009.
23. Okada M, Saio M, Kito Y, Ohe N, Yano H, Yoshimura S, Iwama T and Takami T: Tumor-associated macrophage/microglia infiltration in human gliomas is correlated with MCP-3, but not MCP-1. Int J Oncol 34: 1621-1627, 2009.
24. Platten M, Kretz A, Naumann U, Aulwurm S, Egashira K, Isenmann S and Weller M: Monocyte chemoattractant protein-1 increases microglial infiltration and aggressiveness of gliomas. Ann Neurol 54: 388-392, 2003.
25. Reuss AM, Groos D, Buchfelder M and Savaskan N: The acidic brain-glycolytic switch in the microenvironment of malignant glioma. Int J Mol Sci 22: 5518, 2021.
26. Palazon A, Goldrath AW, Nizet V and Johnson RS: HIF transcription factors, inflammation, and immunity. Immunity 41: 518-528, 2014.
27. Love MI, Huber W and Anders S: Moderated estimation of fold change and dispersion for RNA-seq data with DESeq2. Genome Biol 15: 550, 2014.
28. Kanehisa M and Goto S: KEGG: kyoto encyclopedia of genes and genomes. Nucleic Acids Res 28: 27-30, 2000.
29. Yu G, Wang LG, Han Y and He QY: clusterProfiler: An R package for comparing biological themes among gene clusters. OMICS 16: 284-287, 2012.
30. Subramanian A, Tamayo P, Mootha VK, Mukherjee S, Ebert BL, Gillette MA, Paulovich A, Pomeroy SL, Golub TR, Lander ES and Mesirov JP: Gene set enrichment analysis: A knowledge-based approach for interpreting genome-wide expression profiles. Proc Natl Acad Sci USA 102: 15545-15550, 2005.
31. Hanzelmann S, Castelo R and Guinney J: GSVA: Gene set variation analysis for microarray and RNA-seq data. BMC Bioinformatics 14: 7, 2013.
32. Bindea G, Mlecnik B, Tosolini M, Kirilovsky A, Waldner M, Obenauf AC, Angell H, Fredriksen T, Lafontaine L, Berger A, *et al*: Spatiotemporal dynamics of intratumoral immune cells reveal the immune landscape in human cancer. Immunity 39: 782-795, 2013.
33. Ceccarelli M, Barthel FP, Malta TM, Sabedot TS, Salama SR, Murray BA, Morozova O, Newton Y, Radenbaugh A, Pagnotta SM, *et al*: Molecular profiling reveals biologically discrete subsets and pathways of progression in diffuse glioma. Cell 164: 550-563, 2016.
34. Liu J, Lichtenberg T, Hoadley KA, Poisson LM, Lazar AJ, Cherniack AD, Kovatich AJ, Benz CC, Levine DA, Lee AV, *et al*: An integrated TCGA pan-cancer clinical data resource to drive high-quality survival outcome analytics. Cell 173: 400-416.e11, 2018.
35. Alba AC, Agoritsas T, Walsh M, Hanna S, Iorio A, Devereaux PJ, McGinn T and Guyatt G: Discrimination and calibration of clinical prediction models: Users' guides to the medical literature. JAMA 318: 1377-1384, 2017.
36. Livak KJ and Schmittgen TD: Analysis of relative gene expression data using real-time quantitative PCR and the 2(-Delta Delta C(T)) method. Methods 25: 402-408, 2001.
37. Deng B, Zhu JM, Wang Y, Liu TT, Ding YB, Xiao WM, Lu GT, Bo P and Shen XZ: Intratumor hypoxia promotes immune tolerance by inducing regulatory T cells via TGF-β1 in gastric cancer. PLoS One 8: e63777, 2013.
38. Liao Y, Luo Z, Lin Y, Chen H, Chen T, Xu L, Orgurek S, Berry K, Dzieciatkowska M, Reisz JA, *et al*: PRMT3 drives glioblastoma progression by enhancing HIF1A and glycolytic metabolism. Cell Death Dis 13: 943, 2022.
39. Ding XC, Wang LL, Zhang XD, Xu JL, Li PF, Liang H, Zhang XB, Xie L, Zhou ZH, Yang J, *et al*: The relationship between expression of PD-L1 and HIF-1α in glioma cells under hypoxia. J Hematol Oncol 14: 92, 2021.
40. Wang P, Wan W, Xiong S, Wang J, Zou D, Lan C, Yu S, Liao B, Feng H and Wu N: HIF1α regulates glioma chemosensitivity through the transformation between differentiation and dedifferentiation in various oxygen levels. Sci Rep 7: 7965, 2017.
41. Semenza GL: Targeting HIF-1 for cancer therapy. Nat Rev Cancer 3: 721-732, 2003.
42. Vaupel P and Mayer A: Hypoxia in cancer: Significance and impact on clinical outcome. Cancer Metastasis Rev 26: 225-239, 2007.

43. Tachibana KE, Gonzalez MA and Coleman N: Cell-cycle-dependent regulation of DNA replication and its relevance to cancer pathology. J Pathol 205: 123-129, 2005.
44. Chen J, Xia Y, Peng Y, Wu S, Liu W, Zhang H, Wang T, Yang Z, Zhao S and Zhao L: Analysis of the association between KIN17 expression and the clinical features/prognosis of epithelial ovarian cancer, and the effects of KIN17 in SKOV3 cells. Oncol Lett 21: 475, 2021.
45. Forde PM, Chaft JE, Smith KN, Anagnostou V, Cottrell TR, Hellmann MD, Zahurak M, Yang SC, Jones DR, Broderick S, *et al*: Neoadjuvant PD-1 blockade in resectable lung cancer. N Engl J Med 378: 1976-1986, 2018.
46. Leighl NB, Hellmann MD, Hui R, Carcereny E, Felip E, Ahn MJ, Eder JP, Balmanoukian AS, Aggarwal C, Horn L, *et al*: Pembrolizumab in patients with advanced non-small-cell lung cancer (KEYNOTE-001): 3-year results from an open-label, phase 1 study. Lancet Respir Med 7: 347-357, 2019.
47. Rini BI, Powles T, Atkins MB, Escudier B, McDermott DF, Suarez C, Bracarda S, Stadler WM, Donskov F, Lee JL, *et al*: Atezolizumab plus bevacizumab versus sunitinib in patients with previously untreated metastatic renal cell carcinoma (IMmotion151): A multicentre, open-label, phase 3, randomised controlled trial. Lancet 393: 2404-2415, 2019.
48. Colegio OR, Chu NQ, Szabo AL, Chu T, Rhebergen AM, Jairam V, Cyrus N, Brokowski CE, Eisenbarth SC, Phillips GM, *et al*: Functional polarization of tumour-associated macrophages by tumour-derived lactic acid. Nature 513: 559-563, 2014.
49. Dang EV, Barbi J, Yang HY, Jinasena D, Yu H, Zheng Y, Bordman Z, Fu J, Kim Y, Yen HR, *et al*: Control of T(H)17/T(reg) balance by hypoxia-inducible factor 1. Cell 146: 772-784, 2011.
50. Doedens AL, Phan AT, Stradner MH, Fujimoto JK, Nguyen JV, Yang E, Johnson RS and Goldrath AW: Hypoxia-inducible factors enhance the effector responses of CD8(+) T cells to persistent antigen. Nat Immunol 14: 1173-1182, 2013.
51. Mascanfroni ID, Takenaka MC, Yeste A, Patel B, Wu Y, Kenison JE, Siddiqui S, Basso AS, Otterbein LE, Pardoll DM, *et al*: Metabolic control of type 1 regulatory T cell differentiation by AHR and HIF1-alpha. Nat Med 21: 638-646, 2015.
52. Li MO, Wolf N, Raulet DH, Akkari L, Pittet MJ, Rodriguez PC, Kaplan RN, Munitz A, Zhang Z, Cheng S and Bhardwaj N: Innate immune cells in the tumor microenvironment. Cancer Cell 39: 725-729, 2021.
53. Shaul ME and Fridlender ZG: Tumour-associated neutrophils in patients with cancer. Nat Rev Clin Oncol 16: 601-620, 2019.
54. Tian S, Chu Y, Hu J, Ding X, Liu Z, Fu D, Yuan Y, Deng Y, Wang G, Wang L and Wang Z: Tumour-associated neutrophils secrete AGR2 to promote colorectal cancer metastasis via its receptor CD98hc-xCT. Gut 71: 2489-2501, 2022.
55. Liang J, Piao Y, Holmes L, Fuller GN, Henry V, Tiao N and de Groot JF: Neutrophils promote the malignant glioma phenotype through S100A4. Clin Cancer Res 20: 187-198, 2014.
56. Lanier LL: NK cell recognition. Annu Rev Immunol 23: 225-274, 2005.
57. Saulep-Easton D, Vincent FB, Le Page M, Wei A, Ting SB, Croce CM, Tam C and Mackay F: Cytokine-driven loss of plasmacytoid dendritic cell function in chronic lymphocytic leukemia. Leukemia 28: 2005-2015, 2014.
58. Michel T, Poli A, Cuapio A, Briquemont B, Iserentant G, Ollert M and Zimmer J: Human CD56bright NK cells: An update. J Immunol 196: 2923-2931, 2016.
59. Montaldo E, Vacca P, Moretta L and Mingari MC: Development of human natural killer cells and other innate lymphoid cells. Semin Immunol 26: 107-113, 2014.
60. Goodman A, Patel SP and Kurzrock R: PD-1-PD-L1 immune-checkpoint blockade in B-cell lymphomas. Nat Rev Clin Oncol 14: 203-220, 2017.
61. Krummel MF and Allison JP: CTLA-4 engagement inhibits IL-2 accumulation and cell cycle progression upon activation of resting T cells. J Exp Med 183: 2533-2540, 1996.
62. Hodi FS, O'Day SJ, McDermott DF, Weber RW, Sosman JA, Haanen JB, Gonzalez R, Robert C, Schadendorf D, Hassel JC, *et al*: Improved survival with ipilimumab in patients with metastatic melanoma. N Engl J Med 363: 711-723, 2010.
63. Long GV, Weber JS, Larkin J, Atkinson V, Grob JJ, Schadendorf D, Dummer R, Robert C, Márquez-Rodas I, McNeil C, *et al*: Nivolumab for patients with advanced melanoma treated beyond progression: Analysis of 2 phase 3 clinical trials. JAMA Oncol 3: 1511-1519, 2017.
64. El-Naggar AM, Veinotte CJ, Cheng H, Grunewald TG, Negri GL, Somasekharan SP, Corkery DP, Tirode F, Mathers J, Khan D, *et al*: Translational activation of HIF1α by YB-1 promotes sarcoma metastasis. Cancer Cell 27: 682-697, 2015.
65. Liu ZJ, Semenza GL and Zhang HF: Hypoxia-inducible factor 1 and breast cancer metastasis. J Zhejiang Univ Sci B 16: 32-43, 2015.
66. Xu J, Yang X, Deng Q, Yang C, Wang D, Jiang G, Yao X, He X, Ding J, Qiang J, *et al*: TEM8 marks neovasculogenic tumor-initiating cells in triple-negative breast cancer. Nat Commun 12: 4413, 2021.
67. Qiao K, Liu Y, Xu Z, Zhang H, Zhang H, Zhang C, Chang Z, Lu X, Li Z, Luo C, *et al*: RNA m6A methylation promotes the formation of vasculogenic mimicry in hepatocellular carcinoma via Hippo pathway. Angiogenesis 24: 83-96, 2021.
68. Yue WY and Chen ZP: Does vasculogenic mimicry exist in astrocytoma? J Histochem Cytochem 53: 997-1002, 2005.
69. Huang M, Ke Y, Sun X, Yu L, Yang Z, Zhang Y, Du M, Wang J, Liu X and Huang S: Mammalian target of rapamycin signaling is involved in the vasculogenic mimicry of glioma via hypoxia-inducible factor-1alpha. Oncol Rep 32: 1973-1980, 2014.
70. Li J, Ke Y, Huang M, Huang S and Liang Y: Inhibitory effects of B-cell lymphoma 2 on the vasculogenic mimicry of hypoxic human glioma cells. Exp Ther Med 9: 977-981, 2015.